Contribution of Linear Guest Chains to Relaxational Dynamics in Model Polymer Networks Probed by Time–Domain ^{1}H NMR.

F. Campise[1], L. Roth[2], R. H. Acosta[1], M. A. Villar[2], E. M. Vallés[2], G. A. Monti[1*], D. A. Vega[3*]
[1] *FAMAF – Universidad Nacional de Córdoba, IFEG – CONICET, Córdoba, Argentina*
[2] *Deparment of Chemical Engineering–Planta Piloto de Ingeniería Química, Universidad Nacional del Sur, Bahía Blanca, Argentina and*
[3] *Deparment of Physics–Instituto de Física del Sur (IFISUR), Universidad Nacional del Sur, Bahía Blanca, Argentina*
(Dated: May 29, 2015)

A series of end-linked polymer networks with varying contents of linear guest chains were investigated through swelling and time–domain NMR temperature dependent experiments. Taking advantage of the thermo-rheological simplicity of polydimethylsiloxane polymers, time–temperature superposition (TTS) was employed to expand the characteristic time scales of NMR exploration by about two orders of magnitude. A comparison between swelling data and tube models predictions reveals that NMR captures the dominant features of the equilibrium and the dynamic properties of defects trapped in polymer networks. As high-temperature experiments ensures a complete relaxation of the guest linear chains on the millisecond time scale of the NMR experiments, an accurate description of the network architecture can be provided. Contents of guest chains determined by NMR were found to agree within a $1wt.\%$ accuracy with data of swelling experiments.

PACS numbers: 83.10.Kn, 82.56.Jn, 76.60.-k

Model polymer networks are ideal candidates to assess information on the dynamics of polymer defects and their influence on the elasticity of the system. In an ideal scenario, all polymer chains are crosslinked to the matrix. However, due to a lack of absolute control on the synthesis procedure, a fraction of polymer chains will be either attached to the network by one chain–end only, constituting pendant material, or become unattached "soluble" material [1, 2]. These defects play a crucial role in controlling the dissipative dynamics of polymer networks and therefore have an enormous technological interest, for example in the design of dynamic vibration absorbers or in the tire industry [3]. Usually, the information about the network architecture is indirectly inferred through viscoelastic and swelling experiments combined with different theories that describe equilibrium and dynamic properties [1, 2, 4, 5]. However, a multiplicity of factors, including trapped entanglements, crosslinker fluctuations, non-Gaussian contributions and a myriad of relaxation mechanisms makes the connection among network architecture and response functions quite difficult. It is then very important to develop reliable characterization methods that allow accurate determination of the network parameters that control their response.

NMR is a suitable technique to study complex polymer dynamics. In a microscopic level, the restriction in mobility of polymer chains gives rise to a residual dipolar couplings (RDCs) which provide information on segmental dynamics in terms of an orientation autocorrelation function, respect to the external magnetic field [6, 7]. RDCs can be probed by measuring multiple quantum coherence, in particular, double quantum (DQ NMR) of pendant chains at low concentrations in poly(dimethylsiloxane) (PDMS) networks correlate with elastic shear modulus,

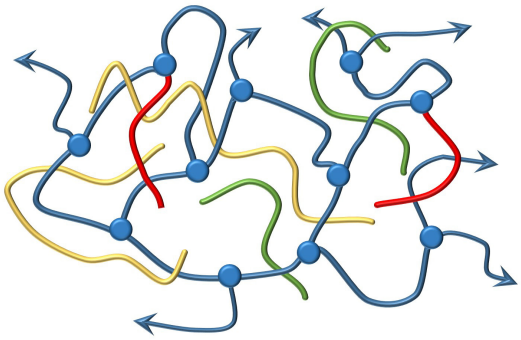

FIG. 1. (Color online) Schematic representation of model PDMS networks obtained via the end-linking technique. Here the trifunctional cross-linkers are indicated with circles, elastic difunctional B_2 chains with blue lines and linear guest chains with yellow lines. Unreacted (green lines) or partialy reacted (red lines) B_2 chains led to soluble and pendant material, respectively.

determined by changes in viscoelastic relaxation times [1]. Unrelaxed topological constrains involving pendant material render a nonzero average dipolar coupling that contributes to the solid-like behavior of the NMR response. For instance, an important increase in the RDCs obtained by DQ NMR was observed as a consequence of the transiently trapped entanglements [8]. In particular, the influence of defects in polymer elasticity can be determined through comparison of DQ NMR and swelling experiments with Miller Macosko calculations [4, 5]. On the other hand, the network fraction of chains that contribute to elasticity at the typical NMR timescales ($\sim$ ms) can be determined by direct inspection of the decay of the transverse magnetization in a multi pulse sequence, such as

in a Carr-Purcell-Meiboom-Gill (CPMG). In this experiment, the elastic fraction, composed by crosslinked chains and trapped defects is described with the Andersson–Weiss model. Relaxed pendant material and free chains decay with the typical exponential behavior associated with liquid–like components [9–11]. There is a linear dependence of the overall magnetization with the solid–like or elastic chain fraction and the contribution of defects that renders the determination of these parameters quite robust.

TABLE I. Networks prepared with different amount of linear guest chains (W_{B0}) of different molecular weights. W_S: amount of soluble material extracted through swelling experiments. ϕ: degree of swelling in toluene.

Network	M_n $[Kg/mol]$	M_w/M_n	r	W_{B0} $[g/g]$	W_S $[g/g]$	ϕ
B_2-00	-	-	0.998		0.004	0.25
B_2-$B_{0,1}$-20	47.8	1.07	1.005	0.196	0.183	0.22
B_2-$B_{0,2}$-05	97.2	1.24	1.035	0.049	0.031	0.24
B_2-$B_{0,2}$-10	97.2	1.24	1.005	0.099	0.057	0.23
B_2-$B_{0,2}$-20	97.2	1.24	1.015	0.196	0.132	0.20

In this work, network architecture and physical entanglement dynamics in polymer networks were investigated by means of time domain NMR (TD–NMR) experiments. A set of model polymer networks were synthesized with different concentration of linear (guest) soluble polymer chains (see details in Table I). Model PDMS networks were obtained by a hydrosylilation reaction between a commercial difunctional prepolymer, α,ω-divinyl poly(dimethylsiloxane)(B_2 : $M_w = 21300 g/mol$; $M_w/M_n = 2.95$)(United Chemical Technology, Inc.) and a trifunctional A_3 phenyltris(dimethylsiloxy)silane crosslinker. Networks were prepared by adding small concentrations of unreactive chains (B_0) to the stoichiometrically balanced reacting mixture of B_2 and A_3 [12, 13]. The unreactive linear chains were obtained by neutralizing the vinyl group chain end of monofunctional polymers, by a hydrosilylation reaction with a monofunctional reagent, pentamethyldisiloxane. The system is then composed of fully reacted B_2 chains that form the network, pendant material consisting of partially reacted B_2 chains that are cross-linked to the network by one end and soluble material from unreacted B_2 and B_0 chains (see scheme of Fig. 1).

Here we take advantage of the difference in molecular weight between the soluble molecules to remove the unreacted B_2 solubles while keeping a small fraction of guest B_0 chains within the network. After reaction was completed, networks were subject to differential extraction of solubles using toluene as solvent [12]. The extraction of solubles was carried out at room temperature for one month, and solvent was replaced every three days. Following extraction, samples were weighed, and the degree of swelling was obtained. Samples were then dried under vacuum at $40°C$ until complete solvent removal was achieved. Dry networks were weighed again, and weight fraction of solubles (W_s) and equilibrium degree of swelling ϕ were calculated (see Table I). After soluble extraction and prior to the NMR experiments, the networks were kept at room temperature for about one month to ensure a homogeneous distribution of guest chains through the network structure.

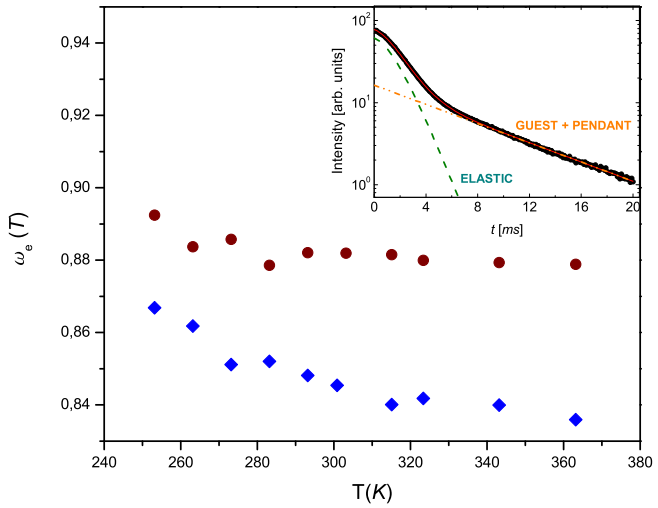

FIG. 2. (Color online) Elastic fraction as a function of the temperature for samples prepared with addition of 5 % of $B_{0,2}$ guest chains (circles) and 20 % of $B_{0,2}$ guest chains (diamonds). The inset shows a characteristic data set with the fitting functions described elsewhere [8].

The dependence of the extraction efficiency on the molecular weight of the free chains is related to the number of physical entanglements in which these chains are involved. Long chains will be subject to a greater amount of conformational rearrangements, decreasing their capacity to diffuse through the gel and thus increasing the extraction time.

In particular, for the systems studied here we have found that the volume fraction ϕ of polymer in networks isothermally swollen up to equilibrium with toluene reach values as low as $\phi \lesssim 0.25$. Under this degree of swelling the B_2 chains can easily escape from the network due to their fast diffusional dynamics. It has been found in entangled polymer melts diluted by theta-solvents that the molar mass between entanglements $Me(\phi)$ depends on polymer concentration ϕ as $M_e(\phi) = M_e^{melt}\phi^{-4/3}$ [14], where M_e^{melt} is the molar mass between entanglements in the melt ($M_e^{melt} \sim 10^4$ g/mol for PDMS). Thus, under equilibrium swelling conditions the effective molecular mass between entanglement for a trapped linear polymer results $M_e(\phi) \sim M_e^{melt} 0.25^{-4/3} \sim 6 M_e^{melt} > M_{B_2}$. Then, in the swollen state the soluble B_2 chains in PDMS networks are completely unentangled and can be easily removed from the network. On the other hand, the B_0 involves a much slower relaxation time and therefore re-

quires longer extraction times. Table I shows the fraction of extracted soluble material (W_s), that corresponds to B_0 chains and unreacted B_2 ones. It can be seen that the nonreactive B_0 guest polymer incorporated into the network during the reaction can not be completely recovered and that the efficiency of the extraction of free chains decreases as its molecular weight increases. For the guest chain molecular weights and concentrations used in this work, the fraction of unextracted material ranges from $\sim (1-6)\%$. Given that the content of both, guest and unreacted B_2 chains are relatively small, there are no self entanglements among these defects. Then, it can be expected that the extraction rates of the the populations of each species become independent of each other. Then, once the reaction and swelling experiments has been completed, the system is composed of fully reacted B_2 chains that form the network, pendant material consisting of partially reacted B_2 chains that are linked to the network by one end and the remaining unextracted fraction of B_0 guest chains (see Table I).

As in the network without linear guest chains (B_2-00) there is a high efficiency in the elimination of solubles B_2, the content of elastic and pendant material can be computed through the fraction of solubles and the Miller-Macosko model [15, 16]. According to this model, the maximum extent of reaction p can be obtained through the fraction of solubles W_s: $W_s = w_a\alpha^3 + w_b\beta^2$, where w_a and w_b are the mass fractions of crosslinkers and difunctional chains, respectively and $\alpha = \frac{1-rp^2}{rp^2}$ and $\beta = 1+rp(\alpha^2-1)$. For this system, the stoichiometric imbalance, r, is computed as $r = f[A_f]_0/2[B_2]_0$, where $[A_f]_0$ and $[B_2]_0$ are the initial concentrations of crosslinkers and difunctional chains, respectively (see Table I). The fractions of elastically active W_e and pendant material W_p can be determined as $W_e = w_a((1-\alpha)^3 + 2\alpha(1-\alpha)^2) + w_b\beta^2$ and $W_p = w_a(3\alpha^2(1-\alpha)+\alpha(1-\alpha)^2)+w_b 2\beta(1-\beta)$. Taking into account the content of solubles, for the network without linear guest chains (B_2-00 in Table I) for this systems results in $p = 0.95$, $W_e \simeq 0.89$ and $W_p \simeq 0.11$.

TABLE II. Experimentally determined parameters for the fraction of guest (W_g^{NMR}), pendant (W_p^{NMR}) and elastic chains (W_e^{NMR}) present in the networks determined by fitting eq.2 to the NMR data.

Network	M_n $[Kg/mol]$	W_g^{sw} $[g/g]$	W_p^{NMR} $[g/g]$	W_e^{NMR} $[g/g]$	W_g^{NMR} $[g/g]$
B_2-00	0.0	-	0.110	0.890	0.00
B_2-$B_{0,1}$-20	47.8	0.01	0.110	0.886	0.004
B_2-$B_{0,2}$-05	97.2	0.02	0.108	0.871	0.021
B_2-$B_{0,2}$-10	97.2	0.04	0.107	0.861	0.032
B_2-$B_{0,2}$-20	97.2	0.06	0.103	0.833	0.064

TD–NMR measurements were carried out on a Bruker Minispec mq20 equipment operating at a resonance frequency of 19.9 MHz for protons. Sample temperature was controlled with a Bruker BVT3000 unit with a stability accuracy of 0.1 K. Slices of 1 mm of sample were centered in 10 mm outer diameter standard NMR glass tube in order to maximize the homogeneity of the radio frequency field. Transverse relaxation decay data were acquired using a compensated CPMG pulse sequence, with an MLEV-4 pulse phase cycling for the refocusing π pulses [17, 18]. For the analysis of the ^{1}H NMR experiments, it was assumed that the transverse magnetization decay can be described as the sum of a solid-like contribution, coming from elastically active chains and transiently trapped entanglements, and a liquid-like contribution, coming from the fraction of relaxed guest and pendant material. A nonlinear leastsquares fitting procedure was used to determine both contributions to the transverse magnetization decay [1]. Figure 2 shows a typical dataset together with the fitting functions (inset).

As the timescale of NMR observation is fixed around 1ms, the transient solidlike contribution coming from the unrelaxed fraction of pendant and guest chains is affected by the temperature. Upon increasing the temperature, an increasing fraction of the chain ends of guest and pendant material loose its configurational memory and becomes isotropic at the timescale of NMR exploration. Then, it should be expected that if the terminal relaxational time of the defects reduces below 1ms the solidlike contribution decays and eventually levels-off at high temperatures. On the other hand, the fraction of elastically active chains generated by the crosslinkers and trapped entanglements cannot modify their contribution to the solidlike response with temperature because these chains are linked to the network through both ends. Then, the temperature-dependant fraction of elastic material $w_e(T)$ determined by NMR can be expressed as:

$$w_e(T) = W_e + g_p(T)W_p + g_g(T)W_g, \qquad (1)$$

where W_e, W_g and W_p represent the fraction of elastic, guest and pendant chains, respectively. Here $g_p(T)W_p$ and $g_g(T)W_g$ are the temperature dependant fractions of unrelaxed pendant and soluble (linear guest) material, respectively.

A decrease of the 1% of the elastic fraction $w_e(T)$ is observed as the temperature increases (see Fig.2)for the network B_2-$B_{0,2}$-05; while for the network B_2-$B_{0,2}$-20 w_e changes form 87 % to almost 83 % for the same temperature range. These different behaviours should be expected if we consider that networks B_2-$B_{0,2}$-05 and B_2-$B_{0,2}$-20 exhibit different fraction of guest chains (see Table II).

Previously, it has been found that during the process of network formation the maximum advance of reaction remains unaffected by the presence of the guest chains [19]. This feature relies on two experimental observations: the

dependance of the equilibrium modulus and width relaxation spectrum with the content of linear guest chains. It was found that the guest chains only have a solvent-like effect on the network elasticity. As in the low frequency regime guest chains cannot contribute to the network elasticity, the scaling of the equilibrium elastic modulus with the concentration of guest chains is consistent with the theory for semidilute theta solutions. In addition, it was also found that upon appropriate rescaling, the relaxation spectrum associated to networks containing different contents of guest chains overlaps quite nicely over a wide range of timescales [19]. Then, the effect of self-entanglements between guest chains is quite small since their distribution of relaxation times is roughly independent of the molar mass content of the unattached material. Based on this observations, it can be considered that the weight fraction of pendant material in the different networks is the same as the corresponding to the system without linear guest chains B_2-00. ($W_p \simeq 0.11$).

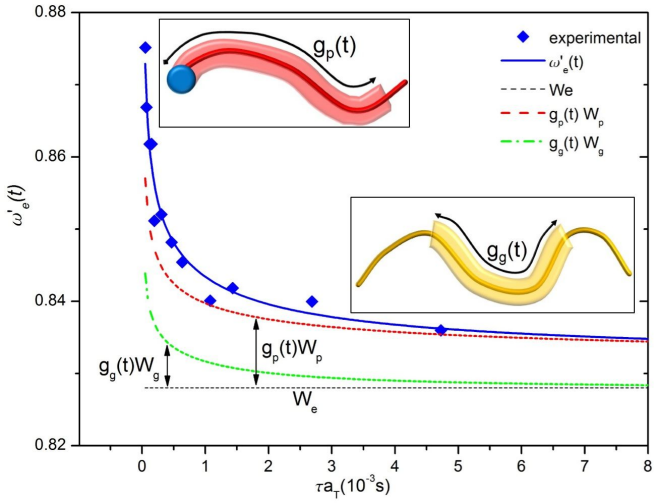

FIG. 3. Elastic fraction determined by NMR as a function of time ($w'_e(t)$) for network B_2-$B_{0,2}$-20. Insets: At the timescale of NMR testing, an unrelaxed fraction of guest $g_g(t)$ and pendant $g_p(t)$ material contributes to the solidlike response.

The tube model theory combined with TTS can be employed to quantify the transient contributions of guest and pendant chains to $w_e(T)$. The fraction of unrelaxed pendant $g_p(t)$ and guest chains $g_g(t)$ can be well described considering a Rouselike dynamics at short times scales combined with a reptation dynamics [20] for the guest chains and arm retraction for the pendant material [2]. Note that within the network there are no dynamic dilution effects and then, the long time dynamics is dictated by "pure reptation" and arm retraction in a Pearson-Helfand potential [2].

Irrespective of the polymer architecture (linear, star shaped or networks), it has been found that PDMS is thermorheologically simple and that the time-frequency

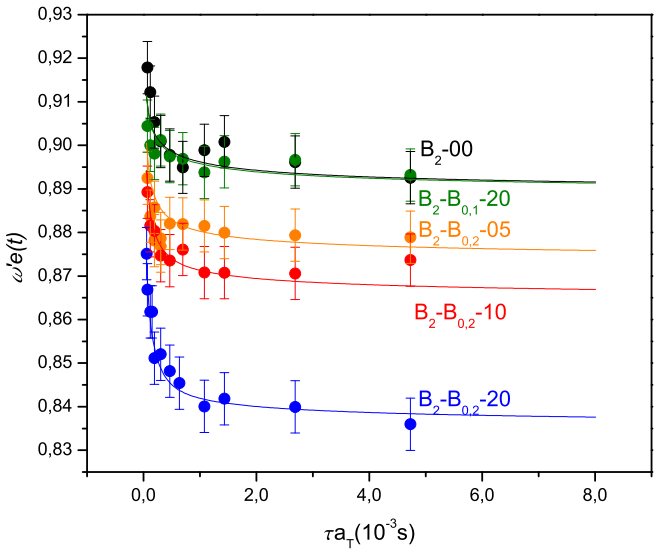

FIG. 4. (Color online) Elastic fraction determined by NMR as a function of time ($w'_e(t)$) for different networks. The solid line is a fitting corresponding to eq. 2

.

shift factors a_T can be equally well described either by the Williams, Landel, and Ferry (WLF) model or the Arrhenius equation [13]. We can then take advantage of the thermorheological simplicity of PDMS to obtain information in the time-domain through data in the temperature domain.

Time-temperature superposition principle was applied to $w_e(T)$ data to obtain the fraction of elastic material as a function of time, $w'_e(t)$. The corresponding horizontal shift factor, a_T, was determined considering an activation energy $E_a \sim 29\ kJ/mol$ [13] and a reference temperature of $T_0 = 313K$. Here we considered a characteristic time of $\tau = 1$ ms [8] (see Fig. (3)). It is worthwhile to mention that within the temperature regime analyzed here, the time-window of exploration increases by almost two orders or magnitude thanks to TTS ($a_{T=253}/a_{T=363} \sim 70$).

Equation (1) is then expressed as:

$$w'_e(t) = W_e + g_p(t)W_p + g_g(t)W_g. \qquad (2)$$

W_e, and W_g were determined by fitting NMR $w'_e(t)$ data by eq. (2). In Fig. 3 we can see that the contribution of the free defects to the elasticity is only relevant at short times. At room temperature the terminal relaxation time for the linear guest chains within the network is $\tau_d \sim 10^{-4}$s and $\tau_d \sim 10^{-3}$s for $B_{0,1}$ and $B_{0,2}$ chains, respectively. Thus, at the $1ms$ timescale of observation the $B_{0,1}$ chains are completely relaxed and cannot contribute to the solidlike response. Observe in Fig. 4 that the relaxation spectrum for networks B_2-$B_{0,1}$-20 and B_2-00 are quite similar. The only difference is a small vertical shift produced by the isotropic contribution of $B_{0,1}$ chains. In the case of the longer linear guest chains $B_{0,2}$, W_g in-

creases with increasing W_{B0} giving rise to a lower value of $w_e(t)$. In this case, $B_{0,2}$ chains are only partially relaxed and contribute to the transient solidlike response. The fitting results of eq. (2) are shown in Table II, where an excellent agreement between the NMR and swelling results for the fraction of guest chains within the network is observed. As pointed out above, although the initial content of guest chains in the networks B_2-$B_{0,1}$-20 and B_2-$B_{0,2}$-20 is the same, the extraction efficiency is quite different due to the differences in molecular weights between the two guest polymers.

In summary, we have shown that slow dynamics of network defects can be directly monitored by NMR spin relaxation of protons as a function of temperature in PDMS model networks. Application of the time-temperature superposition principle to transverse relaxation NMR parameters allows an accurate determination of the contribution of different type of defects to the relaxation processes.

We express our gratitude to the Universidad Nacional del Sur, to Research Councils of Argentina: CONICET, ANPCyT PICT 2010-1096/2274 and SeCyT-UNC which supported this work.

* monti@famaf.unc.edu.ar

[1] R. H. Acosta, D. A. Vega, M. A. Villar, G. A. Monti, E. M. Vallés, Macromolecules 39 (2006) 4788–4792.
[2] D. A. Vega, L. R. Gómez, L. E. Roth, J. A. Ressia, M. A. Villar, E. M. Vallés, Phys. Rev. Lett. 95 (2005) 166002.
[3] H. Yamazaki, M. Takeda, Y. Kohno, H. Ando, K. Urayama, T. Takigawa, Macromolecules 44 (2011) 8829–8834.
[4] W. Chassé, M. Lang, J.-U. Sommer, K. Saalwächter, Macromolecules 45 (2012) 899–912.
[5] S. Schlögl, M.-L. Trutschel, W. Chassé, G. Riess, K. Saalwächter, Macromolecules 47 (2014) 2759–2773.
[6] R. Graf, A. Heuer, H. Spiess, Phys. Rev. Lett. 80 (1998) 5738–5741.
[7] K. Saalwächter, Progress in Nuclear Magnetic Resonance Spectroscopy 51 (2007) 1 – 35.
[8] R. Acosta, G. Monti, M. Villar, E. Vallés, D. Vega, Macromolecules 42 (2009) 4674–4680.
[9] G. Simon, K. Baumann, W. Gronski, Macromolecules 25 (1992) 3624–3628.
[10] J. P. Cohen-Addad, The Journal of Chemical Physics 60 (1974) 2440–2453.
[11] D. Vega, M. Villar, E. Vallés, C. Steren, G. Monti, Macromolecules 34 (2001) 283–288.
[12] M. Villar, M. Bibbó, E. Vallés, Macromolecules 29 (1996) 4072–4080.
[13] M. Villar, V. E.M., Macromolecules 29 (1996) 4081–4089.
[14] R. H. Colby, M. Rubinstein, Macromolecules 23 (1990) 2753–2757.
[15] C. Macosko, D. Miller, Macromolecules 9 (1976) 199–206.
[16] E. Vallés, C. Macosko, Macromolecules 12 (1979) 673–679.
[17] T. Gullion, D. Baker, M. Conradi, Journal of Magnetic Resonance (1969) 89 (1990) 479–484.
[18] K. Saalwächter, B. Herrero, M. López-Manchado, Macromolecules 38 (2005) 4040–4042.
[19] L. Roth, D. Agudelo, J. Ressia, L. Gómez, E. Vallés, M. Villar, D. Vega, European Polymer Journal 64 (2015) 1–9.
[20] S. Milner, T. McLeish, Physical Review Letters 81 (1998) 725–728.